

The 8<sup>th</sup> International Conference on Applied Energy – ICAE2016

## A reduced wide-temperature-range electro-thermal model and thermal parameters determination for lithium-ion batteries

Haijun Ruan<sup>a,b</sup>, Jiuchun Jiang<sup>a,b</sup>, Qun Ju<sup>c</sup>, Bingxiang Sun<sup>a,b,\*</sup>, Gong Cheng<sup>a,b</sup>

*a National Active Distribution Network Technology Research Center, Beijing Jiaotong University, Beijing, 100044, China*

*b Collaborative Innovation Center of Electric Vehicles in Beijing, Beijing Jiaotong University, Beijing, 100044, China*

*c Shandong Lithium-ion Battery Product Quality Supervision and Inspection Center, Zaozhuang, 277100, China*

### Abstract

A reduced wide-temperature-range electro-thermal model, which is based on the frequency-dependent equation, is presented and validated under different frequencies and temperatures. The temperature dependence of resistances and capacitances in a wide temperature range is proposed. In contrast to state-of-the-art electro-thermal models, the presented identification for thermal parameters, which are validated with a very small error, does not require expensive thermal equipment, like calorimeter and is free from the challenges for their installations. Simulation results exhibit good agreement with experiments, where the maximum relative voltage error and temperature error are less than 2.31% and 0.89°C, respectively. The reduced model, thanks to its reliability and simplified characteristic, provides a promising candidate for development of optimal charging strategies in a wide temperature range, for prediction of the electrical and thermal performance of batteries in on-board battery management system.

© 2017 Published by Elsevier Ltd. This is an open access article under the CC BY-NC-ND license

(<http://creativecommons.org/licenses/by-nc-nd/4.0/>).

Peer-review under responsibility of the scientific committee of the 8th International Conference on Applied Energy.

*Keywords:* lithium-ion batteries; wide temperature range; electro-thermal model; thermal parameters determination

### Nomenclature

$L$	Inductance (H)	$R_b$	Ohmic resistance ( $\Omega$ )
$I$	Current through the battery (A)	$C_p$	Polarization capacitance (F)
$R_p$	Polarization resistance ( $\Omega$ )	$R$	Gas constant ( $\text{J} \cdot \text{mol}^{-1} \cdot \text{K}^{-1}$ )
$T$	Battery temperature (K)	$E_{axx}$	Activation energy ( $\text{kJ} \cdot \text{mol}^{-1}$ )
$U_{ocv}$	Open circuit voltage (V)	$T_a$	Ambient temperature ( $^{\circ}\text{C}$ )
$Q_b$	Heat generation rate of the battery (W)	$m$	Battery mass (g)
$R_T$	Thermal resistance ( $\text{g} \cdot \text{K} \cdot \text{W}^{-1}$ )	$A$	Surface area of the battery ( $\text{m}^2$ )
$h$	Heat-transfer coefficient ( $\text{W} \cdot \text{m}^{-2} \cdot \text{K}^{-1}$ )	$C'_p$	Specific heat capacity ( $\text{J} \cdot \text{g}^{-1} \cdot \text{K}^{-1}$ )

## 1 Introduction

The lithium-ion battery (LIB), thanks to its high energy density, long lifetime, and environmental friendliness, is regarded as a favorable candidate for electric vehicles (EVs). The battery temperature plays an important role in LIBs' operation [1]. The elevated temperature may lead to the accelerated fade of the battery life while the enormous impedance at low temperatures leads to substantial reduction in both the pulse power and driving range of EVs [2]. The key to battery performance improvement is to establish a suitable model and manage the temperature properly. Only the LIBs performance is modeled well so that a good thermal management strategy can be presented. Therefore, it is essential to establish a wide-temperature-range electro-thermal model for prediction the electrical and thermal behavior of LIBs.

There are several modeling strategies to predict voltage behavior of LIB. The electrochemical model is complicated while the black box model lacks the description of LIBs performance. The equivalent electrical circuit model, representing the equivalent form of the electrochemical model by using electrical circuit elements, can explicitly characterize battery performance with a good compromise between computation time, simulation accuracy, and parameterization effort [3]. There are two types of equivalent electrical circuit models: one developed from the step-response method [4] and another identified from sinusoidal alternating current (SAC) excitation [5]. The first one is not well suited for high frequency application and cannot properly describe the behavior under alternating current conditions. In contrast, the impedance-based method employs a small SAC excitation, allowing the direct measurement of the system response at any operating point and the measured spectra contain all information about LIB performance.

Sluggish charge-transfer kinetics and decreased solid-state lithium-ion diffusivity within LIBs are found at low temperature. The low-temperature modeling of LIBs is challenging due to the high nonlinear characteristic of model parameters compared to room-temperature modelling. To describe the low-temperature performance of LIBs, a complex mathematical formula considering the effect of the temperature is introduced for battery modelling in [6]. Moreover, only the discharge behavior is included in the model in [6] and only the low-temperature performance is described. Although the model in [7] is simplified, the current used to validate for the reduced model is much lower. Moreover, the model only describes the charge behavior under low temperature. Therefore, developing a simplified and accurate model, considering wide temperature range, is essential for LIBs' applications in various conditions.

In this work, a reduced wide-temperature-range electro-thermal model, which is validated with time-domain data, is presented to accommodate the performance of LIB under different frequencies and temperatures. For most of the traditional electro-thermal models [8], the thermal parameters are determined through a dedicated and expensive test bench including thermal test equipment, like calorimeter, which makes the modeling process of LIB complicated and time-consuming [9]. However, thermal parameters of the proposed model, which are validated with a very small error, are estimated from data measured under the SAC excitation and the cooling process using the common experimental workbench, which is simple and independent of expensive instruments. Simulation results from the model show good agreement with experiments, where the maximum relative voltage error and temperature error are less than 2.31% and 0.89°C respectively. The reduced model, thanks to its reliability and attractive simplicity, yields a promising candidate for application in on-board battery management system.

## 2 Electro-thermal coupled model

### 4.1 Electrical model

Fig.1 shows the reduced and accurate model, which is improved from the literature [10]. The values of resistance ( $R_p(f,T,S)$ ) and capacitance ( $C_p(f,T,S)$ ) depend on SAC frequency ( $f$ ), which are based on the FD equation as described by Eq.(5) in the appendix, battery temperature ( $T$ ) and state of charge ( $S$ ). Model parameters of polarization are dependent on the battery temperature as expressed by Eq.(1). The temperature dependence is piecewise linear approximation, which represents different prominent electrochemical reaction at different temperature range.

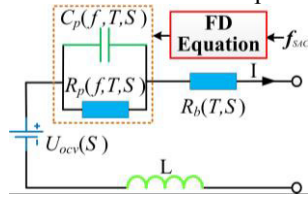


Fig. 1. the reduced equivalent electrical circuit model

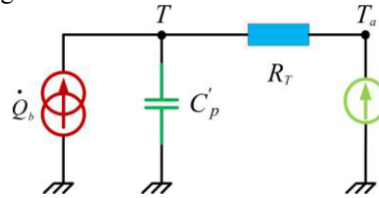


Fig. 2. equivalent electric thermal model

$$\begin{cases} \ln[R_x(T)] = \frac{E_{arx}}{1000 \times R} \times \frac{1000}{T} + \ln b_{rx} \\ \ln[C_x(T)] = -\frac{E_{acx}}{1000 \times R} \times \frac{1000}{T} + \ln b_{cx} \end{cases} \quad (1)$$

### 2.2 Thermal model

Battery temperature is assumed to be uniform and lumped thermal model is developed. The improved equation (2) can be deduced from first law of thermodynamics as shown in Fig.2.

$$\dot{Q}_b = C'_p \frac{dT}{dt} + \frac{T - T_a}{R_T} \quad (2)$$

When the heat generation rate is zero, namely no input current, Eq. (2) can be given as

$$\tau_T = R_T C'_p = \frac{m C'_p}{Ah} = \frac{(T_a - T) dt}{dT} \quad (3)$$

During the cooling of LIB, the thermal time constant can be estimated. Battery temperature ( $T_1$ ) can be recorded when the battery is subjected to a symmetrical SAC while the estimated temperature ( $T_2$ ) can be obtained based on Eq. (2). Then the thermal parameters, namely  $C'_p$  and  $h$ , can be calculated, which does not require expensive and complex equipment, such as ARC and their associated challenging installations.

$$\text{Min} \left[ \sum (T_1(t) - T_2(t))^2 \right] \quad (4)$$

In addition,  $C'_p$  can be obtained by specifically designed experiments, where the adiabatic condition on battery surfaces is created using ARC. Combining the electrical model and the thermal model, a reduced wide-temperature-range electro-thermal (RWET) model is presented.

### 3 Experimental

The tested batteries with NCM cathode material and the experimental platform are the same as that presented in the literature [10]. After soaked at a certain temperature, such as  $-20^\circ\text{C}$  for more than 5h, the EIS is carried out and then the LIBs are subjected to the current with different frequencies. The same experimental process is conducted at  $-15^\circ\text{C}$ ,  $-10^\circ\text{C}$ ,  $-5^\circ\text{C}$ ,  $0^\circ\text{C}$ ,  $5^\circ\text{C}$ ,  $10^\circ\text{C}$ ,  $17^\circ\text{C}$ ,  $25^\circ\text{C}$ ,  $32^\circ\text{C}$ ,  $40^\circ\text{C}$ ,  $47^\circ\text{C}$ ,

and 55°C. To measure the thermal parameters, the batteries were kept under 31.2°C for more than 5h in ARC. Then, the heater in ARC is started to warm batteries up to 60.1°C with the rate of 0.2°C/min. The battery was thermally equilibrated in a climate chamber at 55°C and 25°C, and then was put into the incubator for cooling, where the environmental temperature was held at 25°C and -20°C, respectively.

### 4 Results and discussions

#### 4.1 Model extraction

The natural logarithms of fitting parameters, which are from fitting the polarization resistance and polarization capacitance based on the FD equation, vary linearly with the reciprocal of the absolute temperature as shown in Fig. 3 under two temperature ranges.

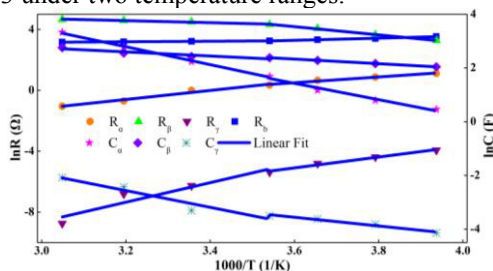


Fig. 3. temperature dependence of the resistance and capacitance parameters under -20~55°C.

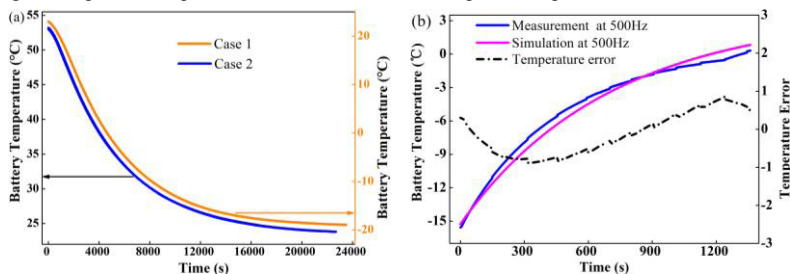


Fig. 4. temperature evolution (a) cooling (b) SAC excitation with 10A at 500Hz

Table 1. Thermal parameters

	Case 1	Case 2	Case 3	Average
$\tau_T(s)$	119.163	136.434	136.261	127.799
$C'_p(J \cdot g^{-1} \cdot K^{-1})$	1.388	1.406	1.419	1.404
$h(W \cdot m^{-2} \cdot K^{-1})$	11.678	10.305	10.414	10.986

The thermal time constant ( $\tau_T$ ) is calculated using the temperature data displayed in Fig. 4(a) in the range from 55°C to 25°C (Case 1 and Case 2) and from 55°C to 25°C (Case 3). When the battery is subjected to SAC with 10A at 500Hz, battery temperature rises gradually as shown in Fig. 4(b). The thermal parameters can be evaluated based on Eq. (3) and (4) in MATLAB. The specific heat capacity ( $C'_p$ ) is 1.404 J·g<sup>-1</sup>·K<sup>-1</sup> and the heat transfer coefficient (h) is 10.986 W·m<sup>-2</sup>·K<sup>-1</sup> as shown in Table 1, where the least sum of the square of errors between the estimated and measured temperatures is obtained.

#### 4.2 Verification at different frequencies

The validations were carried out with steady-state SAC excitation at different frequencies under -20°C. Voltage results under 5A and 50Hz for measurement and simulation are shown in Fig.5 (a). It is observed

that presented models can predict battery voltage with a high accuracy as shown in Fig. 5 (b). Table 2 lists simulation errors of the RWET model at various frequencies. It is concluded that the presented model has a very comparable performance with the mean error and the maximum relative error of less than 18.71mV and 1.88%, respectively. The mean errors and maximum relative errors of the RWET model are all very small, implying that the presented model can accurately emulate the voltage behavior of LIB.

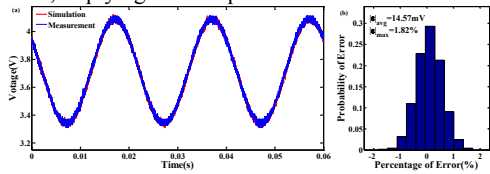


Fig. 5. (a) voltage evolution at 50Hz under -20°C (b) error distribution of RWET model simulation

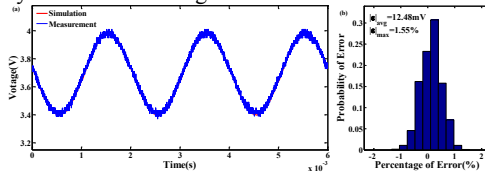


Fig. 6. (a) voltage evolution at 500Hz under 17°C (b) error distribution of RWET model simulation

4.3 Verification at different temperatures

Furthermore, Fig.6 displays simulation results and experimental data at 17°C and Table 2 lists simulation errors under various temperatures. It can be concluded that the mean errors of the RWET model are less than 17.86mV and the maximum relative errors are less than 2.31% at four different temperatures. The well matched results confirm that simulation results of the presented model are highly consistent with terminal voltage profiles obtained from the experimental data.

Table 2. Simulation errors at various temperatures

Temperature(°C)	-20		-5		17		32		47	
Frequency(Hz)	$ \epsilon _{avg}(mV)$	$ \epsilon _{max}(\%)$	$ \epsilon _{avg}(mV)$	$ \epsilon _{max}(\%)$	$ \epsilon _{avg}(mV)$	$ \epsilon _{max}(\%)$	$ \epsilon _{avg}(mV)$	$ \epsilon _{max}(\%)$	$ \epsilon _{avg}(mV)$	$ \epsilon _{max}(\%)$
50	14.57	1.82	11.4	1.41	11.79	1.34	11.46	1.43	12.84	1.54
500	18.71	1.88	11.18	1.44	12.48	1.55	11.21	1.44	11.93	1.57
5000	16.13	1.84	17.48	2.13	16.34	1.96	17.86	2.31	17.68	2.25

4.4 Verification for temperature-rise of LIB

The temperature evolution and error distribution with SAC excitation of 10A and 500Hz are shown in Fig.7. Obviously, there is a close match between battery temperatures extracted from experimental data and simulation results of the presented model, where the maximum absolute errors are less than 0.89°C. Besides, the simulation results at different initial temperatures explain that it predicts accurately the thermal behavior of LIBs, indicating the precision of the extracted thermal parameters as well as their identification method.

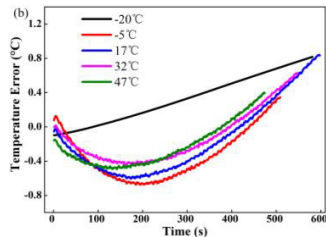
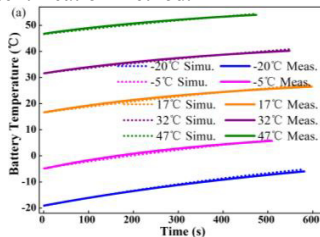


Fig. 7. (a) temperature evolution (b) error distribution at different initial temperatures

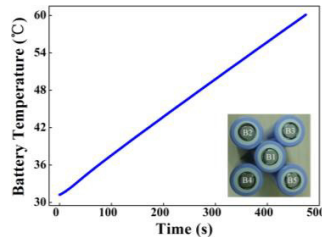


Fig. 8. temperature evolution during heating

4.5 Discussions

The five batteries are arranged as shown in Fig.8. The circular anode surface of the inner battery (B1) is wrapped with resistance heating wire and the cathode of the round battery (B2) is connected with a

temperature sensor. The heating power of ARC is recorded in real-time and the specific heat capacity is calculated, with  $C'_{p0}$  equal to  $1.421\text{J}\cdot\text{g}^{-1}\cdot\text{K}^{-1}$ . Accordingly, the heat transfer coefficient ( $h$ ) is obtained from the thermal time constant. The relative deviations of simulation, which is 1.3%, are small enough to meet the application's requirement, implying that the presented estimation methodology can precisely predict the thermal parameters with good robustness.

## 5 Conclusions

In this study, a simplified RWET model for LIB, which captures accurately both electrical and thermal performances under a wide temperature range, is developed with the following features:

(a) Based on the strong influence of temperature on polarization resistances and capacitances, the temperature dependence of resistances and capacitances is presented in a wide temperature range. The wide-temperature-range simulation results exhibit good agreement with experiments, where the maximum relative voltage error and temperature error are less than 2.31% and 0.89°C, respectively.

(b) Identification for thermal parameters does not require expensive thermal test equipment, like calorimeter, and is free from challenges for their installations. A new method to evaluate thermal parameters is proposed based on data measured under SAC excitation and a simple thermal test. The validation shows that the determined parameters of the model are highly accurate.

## References

- [1] Lin X, Perez H E, et al. A lumped-parameter electro-thermal model for cylindrical batteries[J]. *J. of P. S.*, 2014, 257:1–11.
- [2] Liao L, Zuo P, Ma Y, et al. Effects of temperature on charge/discharge behaviors of LiFePO<sub>4</sub>, cathode for Li-ion batteries[J]. *Electrochimica Acta*, 2012, 60:269-273.
- [3] Dong T K, Kirchev A, et al. Dynamic Modeling of Li-Ion Batteries Using an Equivalent Electrical Circuit[J]. *J. of the Electrochemical Society*, 2011, 158(3):A326-A336.
- [4] Jiang J, Liu Q, Zhang C, et al. Evaluation of Acceptable Charging Current of Power Li-Ion Batteries Based on Polarization Characteristics[J]. *IEEE Transactions on Industrial Electronics*, 2014, 61:6844-6851.
- [5] Moss P L, Au G, Plichta E J, et al. An Electrical Circuit for Modeling the Dynamic Response of Li-Ion Polymer Batteries[J]. *J. of the Electrochemical Society*, 2008, 155(155):A986-A994.
- [6] Yi J, Kim U S, Shin C B, et al. Modeling the temperature dependence of the discharge behavior of a lithium-ion battery in low environmental temperature [J]. *J. of Power Sources*, 2013, 244:143-148.
- [7] Remmlinger J, Tippmann S, Buchholz M, et al. Low-temperature charging of lithium-ion cells Part II: Model reduction and application [J]. *Journal of Power Sources*, 2014, 254(15):268-276.
- [8] Hu Y, et al. Electro-thermal battery model identification for automotive applications[J]. *J. of P. S.*, 2011, 196(1):449-457.
- [9] Mao J, Tiedemann W,. Simulation of temperature rise in Li-ion cells at very high currents[J]. *J. of P. S.*, 2014, 271:444-454.
- [10] Jiuchun Jiang, et al. A reduced low-temperature electro-thermal coupled model for lithium-ion batteries[J]. *Applied Energy*, 2016, 177:804-816.

## Appendix

The frequency-dependent (FD) equation in RWET model is expressed as ( $Z_p$  represents resistance ( $R_p(f)$ ) or capacitance ( $C_p(f)$ ):

$$Z_p = \frac{Z_\alpha}{Z_\beta + f} + Z_\gamma \quad (5)$$